Vacuum 106 (2014) 16–20

Contents lists available at ScienceDirect

Vacuum

journal homepage: www.elsevier.com/locate/vacuum

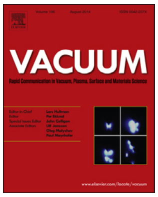

Effects of Zr addition on properties and vacuum arc characteristics of Cu-W alloy

Xiaohong Yang*, Juntao Zou, Peng Xiao, Xianhui Wang

Shaanxi Key Laboratory for Electrical Materials and Infiltration Technology, School of Materials Science and Engineering, Xi'an University of Technology, Xi'an 710048, China

ARTICLE INFO

Article history:
Received 21 January 2014
Received in revised form
4 March 2014
Accepted 5 March 2014

Keywords:
CuZrW alloy
Properties
Vacuum arc
Arc erosion

ABSTRACT

In the present research, CuZrW alloys were prepared by CuZr alloys infiltrating W skeleton technique. After the solution and aging treatment, the properties, microstructures and vacuum arc characteristics of CuZrW alloys were studied. The results show that the electrical conductivity and hardness of CuZrW alloys is increased slightly after the solution and aging treatment. The vacuum arcs on the CuZrW cathode materials surface were scattered effectively because the element Zr strengthens the Cu/W interphase and the rich Cu phase zones. And the molten copper splash is slight and fine dispersed erosion craters were formed on the cathode surface during the vacuum electrical breakdown. In the vacuum discharge course, CuZrW alloys exhibit excellent arc stability, the chopping current is lower and the arc life-span is longer than that of Cu-W alloys.

1. Introduction

Cu-W alloys are widely used as the heavy-duty electrical contact materials due to their outstanding properties of high electrical and thermal conductivity, resistance to arc erosion and to welding [1–4]. With the development of the miniaturized and high-power vacuum interrupter, the W-Cu electrical contact materials used as vacuum switchers are required to improve the electrical properties further, especially for lower chopping current and higher resistance to arc erosion. Therefore, extensive studies have been undertaken to investigation on the electrical properties and vacuum arc characteristics of W-Cu contact materials [5–7].

Due to the mutual insolubility and low wettability between W and Cu, no phase can be seen between tungsten and copper in the microstructure of Cu-W alloys [8,9], Cu/W interphase is difficult to achieve complete densification, and the interfacial bond is weak. In addition, the work function of copper phase is lower than that of tungsten phase. So, the previous investigations [6,7] indicate that the vacuum breakdown position on the surface of Cu-W alloys occurs mainly on the rich Cu phase and Cu/W interfacial zones, where liquid copper is sputtered intensely and larger cathode craters are formed. This phenomenon can accelerate the centralization arc erosion and the presence of cracks along Cu/W interphase. In the present investigation, a small amount of zirconium were selected to add into Cu-W alloy, and the CuZrW alloys were prepared by the infiltration process which CuZr alloys were infiltrated into the sintered W skeleton. At elevated temperature, the solute element zirconium in the molten copper can be partly dissolved in tungsten according to the Zr-W binary phase diagram [10], and the residual zirconium can be precipitated in the copper matrix during cooling to room temperature according to the Cu–Zr binary phase diagram [11]. And then the Cu/W interface and rich copper phase are strengthened through the dissolution and precipitation process. Therefore, the microstructures, physical properties, and electrical properties and vacuum arc characteristics of CuZrW alloys were investigated in this paper.

2. Experimental procedures

Pure (>99.9%) Cu, Zr were used to prepare CuZr alloys in melting furnace at Ar atmosphere. These different contents of CuZr alloys (1.0%, 2.0%, 3.0%, 4.0% mass fraction of Zr in copper) were melted separately at 1250 °C for 1 h, and cooled to room temperature with furnace cooling. Subsequently, these CuZr alloy ingots were machined to remove various casting defects, and were cleaned and dried to be used in the followed infiltration process.

Pure tungsten powder (>99.8%, 4–6 μm) and Ni powder (0.9% mass fraction of W) were wet mixed in a V-type mixing machine for 6 h. The mixed powders were compacted in a hydrostatic machine at the pressure of 340 MPa to obtain green compacts with a relative

---

* Corresponding author. Tel.: +86 29 82312185; fax: +86 29 82312181.
E-mail addresses: yangxh2000@126.com, yangxh@xaut.edu.cn (X. Yang).

http://dx.doi.org/10.1016/j.vacuum.2014.03.009
0042-207X/

density of 65%. Cleaned CuZr alloy blocks were first placed above each compact then put into the graphite crucibles together. Subsequently, these samples in the crucibles were sintered and infiltrated in a sintering furnace at hydrogen atmosphere. W skeletons were sintered at 1000 °C for 2 h, CuZr alloys blocks were infiltrated at 1400 °C for 2 h, and finally furnace cooling was used. The solution treatment of these samples were conducted at 1000 °C for 1 h, and followed by water quenching. All samples of the aging treatment were carried out at 450 °C for 4 h. The electrical conductivity of these samples was tested by an FQR-7501 vortex conduct-meter, and hardness was tested by a Brinell tester.

The vacuum breakdown experiment of different samples were carried in a high vacuum chamber [12,13], which can reach 1.0×10^{-6} Pa by using a sputter ion pump. After polishing, the sample was put in a sample holder as a cathode. Above the cathode, there is a pure tungsten rod with a tip of 0.5 mm as an anode. Then, the voltage of 10 kV was applied to the vacuum gap between the sample and a pure tungsten tip. The cathode was moved to anode at a speed of 0.2 mm/min until the vacuum gap was broken down. A Phantom V9.0 digital high-speed video camera with a Nikon Micro-105 mm lens was set outside a window of the chamber to record vacuum arcs generated between anode and cathode. In this work, the set resolution of the camera is 192 × 64 dpi, and a sample rate is 50,000 frames per sec. The current-time curve of discharge was recorded by a TDS-2024 of Tektronics oscillograph at the same time, the arc chopping current and the arcing time can be directly measured by the curve.

The surface morphologies of samples after electrical breakdown were characterized by an JSM-6700F scanning electron microscopy (SEM). The microstructure and composition of CuZrW alloys were examined by scanning electron microscopy (SEM) equipped with energy dispersive spectrometry (EDS). The compositional definition of interfacial regions were analyzed through line scanning by the electron probe microanalysis (EPMA) attached to SEM.

3. Results and discussion

3.1. Static properties and microstructures of CuZrW alloys with different contents of Zr

The CuZrW alloys infiltrated by CuZr alloys with different contents of Zr addition were subsequently conducted the solution and aging treatment, the electric conductivity and hardness of these alloys at the different conditions were tested, and the measured results were listed in the Table 1. It can be seen that the electric conductivity was decreased, and the hardness was increased with the increase of Zr addition. In addition, compared with the infiltrated condition, both the electric conductivity and hardness of these CuZrW alloys were all increased after the solution and aging treatment.

Fig. 1 shows the EPMA line scanning analyses of the microstructures of CuZrW alloys after the solution and aging treatment. The bright gray phase was the W skeleton, and the dark phase was infiltrated CuZr alloys as shown in Fig. 1(a). It can be seen from Fig. 1(a) and (b) that element Zr was appeared both Cu phase and W phase, and the content of element Zr in W phase is higher than the content in the Cu phase. This indicates that a larger amount of element Zr in CuZr alloys was diffused and dissolved into the W skeletons in the infiltration and the solution process, the remaining element Zr was precipitated in copper matrix during the aging treatment, and the metallurgical bonding interphase of Cu/W were obtained through above the mass transfer and metallurgy processes. Therefore, the electric conductivity of these CuZrW alloys increase due to the precipitation of Zr from the copper matrix, and the hardness increase owing to the aging strengthening of copper matrix and the interfacial strengthening of Cu/W boundaries in the aging treatment process.

Table 1
The electric conductivity and hardness of CuZrW alloys with different contents of Zr at different conditions.

Zr contents in copper (wt%)	Electric conductivity (IACS%)		Hardness (HB)	
	Infiltrated condition	Solution and aged condition	Infiltrated condition	Solution and aged condition
1%	36.0	39.1	182	235
2%	35.3	37.6	187	249
3%	34.8	36.7	196	264
4%	33.3	35.2	210	273

3.2. Arc erosion morphologies of CuZrW alloy after 50 times electrical breakdowns

Fig. 2(a) and (b) shows the surface SEM morphologies of CuW alloy and CuZrW alloy after 50 times vacuum electrical breakdowns, respectively. It can be seen that the arc erosion area of the surface of CuZrW alloy is significantly greater than that of CuW alloy. As for CuW alloy, most serious arc erosion occurs in the central region below the anode tungsten tip where the cathode spots was overlapped together and more deeper craters were formed. This indicates that the arc spots were moved repeatedly in a very small area. Consequently, surfaces roughness worsens with increases in breakdown times. As for CuZrW alloy with 3wt.% Zr addition, the spots are scattered from center to fringe zones, and thus smaller and flatter craters are formed after 50 times vacuum electrical breakdowns. These results indicate that arc is dispersed by the addition of element Zr in the vacuum breakdown process, so the arc erosion areas are expanded and the ablation surface roughnesses are decreased.

3.3. Characteristics of cathode spots of the first breakdown

In order to reveal the effect of Zr addition on the arc erosion mechanism of CuW alloy, a digital high-speed video camera was employed to record the motion of cathode spots generated by vacuum arc during the first vacuum breakdown. Figs. 3 and 4 show the images of cathode spot motions on the surface of CuW alloy and CuZrW alloy, respectively. In addition, the photos of the moving spots captured at different time 0 μs, 200 μs, 350 μs, and 800 μs are separately shown in Figs. 3 and 4(a)–(d). It can be seen that the cathode spot of CuW alloy is always only one bright spot, the cathode spot has no obvious division, and the cathode spot becomes smaller and darker until is extinguished in the whole discharge time. However, the cathode spot of CuW alloy is divided when the discharge time is 200 μs, and the spots are constantly split into several secondary cathode spots with the increase of discharge time. Compared Fig. 3 with Fig. 4, it indicates that the element Zr addition in CuW alloy can scatter vacuum arcs. These divided cathode spots can disperse the enormous arc energy produced in the breakdown process to some extent, and thus the concentration arc erosion can be avoided for CuZrW alloy.

In order to determine the first breakdown phases and places of vacuum arcs on the surface of different materials, the surface morphologies of CuW alloy and CuZrW alloy after the first electrical breakdown were examined by SEM, as shown in Fig. 5. It can be seen that the copper phase is the dielectric weak phase for these alloys because the arc firstly occurs in the rich copper zones. For CuW alloy, it is indicated that almost all breakdowns occurs in the copper phase and the boundaries of Cu/W, where a mass of copper was sputtered intensely, and so larger, deeper and centralized